Contents lists available at ScienceDirect

Biochemistry and Biophysics Reports

Increased level of phosphorylated desmin and its degradation products in heart failure

Marion Bouvet [a], Emilie Dubois-Deruy [a], Tchilabalo Dilezitoko Alayi [b], Paul Mulder [c], Myriam El Amranii [b], Olivia Beseme [a], Philippe Amouyel [d], Vincent Richard [c], Stanislas Tomavo [b], Florence Pinet [a,*]

[a] INSERM, U1167, University Lille, Institut Pasteur de Lille, F-59000 Lille, France
[b] University Lille, CNRS UMR8204, INSERM, U1019, Institut Pasteur de Lille, Plateforme de Protéomique et des Peptides Modifiés (P3M), F-59000 Lille, France
[c] INSERM, U1096, University of Rouen, Institute for Research and Innovation in Biomedicine, F-76000 Rouen, France
[d] INSERM, U1167, University Lille, Institut Pasteur de Lille, Centre Hospitalier Régional et Universitaire de Lille, F-59000 Lille, France

ARTICLE INFO

ABSTRACT

Although several risk factors such as infarct size have been identified, the progression/severity of heart failure (HF) remains difficult to predict in clinical practice. Using an experimental rat model of ischemic HF and phosphoproteomic technology, we found an increased level of phosphorylated desmin in the left ventricle (LV) of HF-rats. The purpose of the present work is to assess whether desmin is a circulating or only a tissue biomarker of HF. We used several antibodies in order to detect desmin, its proteolytic fragments and its phosphorylated form in LV and plasma by western blot, phosphate affinity electrophoresis, mass spectrometry and immunofluorescence. Plasma was treated with combinatorial peptide ligand library or depleted for albumin and immunoglobulins to increase the sensitivity of detection. We found a 2-fold increased serine-desmin phosphorylation in the LV of HF-rats, mainly in the insoluble fraction, suggesting the formation of desmin aggregates. Desmin cleavage products were also detected in the LV of HF rats, indicating that the increased phosphorylation of desmin results in more susceptibility to proteolytic activity, likely mediated by calpain activity. The native desmin and its degradation products were undetectable in the plasma of rat, mouse or human. These data suggest the potential of serine-phosphorylated form of desmin and its degradation products, but not of desmin itself, as tissue but not circulating biomarkers of HF.

1. Introduction

Chronic heart failure (HF) remains a major cause of illness and death and its prevalence is increasing with a high rate of morbidity and mortality [1]. Despite major significant advances, HF remains a therapeutic challenge, and several adverse consequences of HF are still poorly controlled. New prognostic or diagnostic biomarkers of HF are still important to find and proteomic approaches may be useful [2].

Novel determinants of post-myocardial infarction (MI)-HF were already revealed by previous proteomic [3] and phosphoproteomic [4] approaches. We recently discovered that HF is associated with decreased levels of myocardial and plasma serine[208]-phosphorylated troponin T (TnT) in an experimental rat model of HF and

confirmed the same decrease in plasma of patients with high LV remodeling post-MI, suggesting that the level of circulating phosphorylated TnT could be new biomarker of LV remodeling and may help to predict the development of HF after MI [5]. More recently, seven proteins were found differentially expressed in cardiac tissues in a mouse model of HF (calcineurin transgenic mice) and their presence in plasma of HF mouse models but also in HF patients have been investigated [6]. From these candidate biomarkers highlighted, desmin was found to be detected in plasma from mouse (~45 kDa) and human (~22 kDa) species, suggesting the potential of circulating desmin as biomarker of HF. Desmin is one of the five major groups of intermediate filament (IFs) that packs myofibrils and mitochondria together inside the cardiomyocyte and establishes a crucial link with the sarcolemma and nuclear membranes. Desmin is a 53 kDa protein that forms a cytoskeletal network across the muscle fiber bordering at the plasma and nuclear membrane and is particularly localized to the Z-band [7]. Desmin has been described as a major integrator of IF

network raising the question of how desmin can be secreted into the blood.

Our experimental rat model of ischemic HF offers an easy access to heart tissue and plasma from the same animal and we have identified increased phosphorylation of desmin in LV of HF-rats compared to the sham-rats (Supplemental Fig.1 and Supplemental Table 1).

It was recently reviewed that during the development of HF, heart homeostasis should be maintained by the balance between protein synthesis and degradation [8]. Three major degradation systems have been identified, namely the calpain systems, autophagy and the ubiquitin proteasome. Interestingly, desmin is the target of proteolytic degradation systems and of post-translation modifications (PTMs), such as phosphorylation and ubiquitinylation [9].

Desmin as other cytoskeletal proteins has been hypothesized to reproducibly degenerate into the same degradation products, upon the activity of the Ca^{2+} dependent calpains [10] that have been localized in heart mitochondria [11]. These recent data suggest that calpains in the heart could be involved in degradation of desmin that could be secreted into the blood.

The purpose of this work performed in a rat model of HF following MI was to characterize (1) whether cardiac desmin is a target of the same or other sites of phosphorylation than those previously described; (2) its susceptibility to degradation proteolytic systems in this experimental model of HF post-MI and, (3) its potential as being a tissue or circulating biomarker of ischemic HF.

2. Materials and methods

2.1. Animal models

All animal experiments were performed according to the Guide for the Care and Use of Laboratory Animals published by the US National Institutes of Health (NIH publication NO1-OD-4-2-139, revised in 2011). Animals were used and experimental protocols performed under the supervision of a person authorized to perform experiments on live animals (F. Pinet: 59-350126, exp. date: 22 June 2016). Approval was granted by the institutional ethics review board (CEEA Nord Pas-de-Calais N°242011, January 2012).

Before surgery, rats were anaesthetized (sodium methohexital, 50 mg/kg intraperitoneally (IP)), while analgesia was administered before (xylazine 5 mg/kg IP) and 1 h after surgery (xylazine 50 mg/kg subcutaneously) as described [12]. Anesthesia and sedation were controlled by monitoring heart rate. MI was induced in 10-week-old male Wistar rats (n=11) (Janvier, Le Genest *St* isle, France) by ligation of the left anterior descending coronary artery [12,13]. Haemodynamic and echocardiographic measurements were taken 2 months after surgery, followed by heart excision, as previously described [4,14].

Hearts and blood from 14-week-old C57/BL6 mices (n=3) were collected after euthanasia by an overdose of sodium pentobarbital (50 mg/kg IP).

2.2. Primary cultures of neonate rat cardiomyocytes

Primary cultures of rat neonatal contractile cardiac myocytes (NCMs) were prepared from heart ventricles of 1- or 2-day-old rats, killed by decapitation, minced in a balanced salt solution containing 20 mmol/L HEPES, 120 mmol/L NaCl, 1 mmol/L NaH_2PO_4, 5.5 mmol/L glucose, 5.4 mmol/L KCl, and 0.8 mmol/L $MgSO_4$ [pH 7.4] as previously described [15]. NCMs were seeded at a density 8×10^5 cells/well in 6-well plates coated with 0.01% of collagen (Sigma-Aldrich) and cultured in a medium containing 4 parts of DMEM and 1 part of Medium199, 10% horse serum (Life Technologies), 5% foetal bovine serum (ATCC), 1% penicillin and

streptomycin (10,000 U/mL, Life Technologies) for 7 days at 37 °C under 5% CO_2 atmosphere.

2.3. Plasma preparation

Blood samples from systolic HF-human male patients of ischemic origin (LVEF < 45%) with NYHA class 2 (INCA, CP 98/94 of 5 November 1998, CHRU Lille-FRANCE) [16], HF-rat and from control mouse were collected in EDTA-treated tubes and then centrifuged for 15 min at 1600 g to remove cells and platelets. After centrifugation, the plasma (resulting supernatant) was collected, aliquoted and stored at –80 °C. Plasmas were treated either by albumin and IgG (Alb/IgG) depletion or combinatorial peptide ligand library (CPPL) as previously described [17].

2.4. Tissue fractionation

LV proteins were extracted from 40 mg of frozen tissue (after removing the infarcted area) with Dounce-Potter homogenization into ice-cold RIPA buffer (50 mmol/L Tris [pH7.4], 150 mmol/L NaCl, 1% Igepal CA-630, 50 mmol/L deoxycholate, and 0.1% SDS) containing *anti*-proteases (Complete™ EDTA-free, Roche Diagnostics), serine/threonine and tyrosine protein phosphatase inhibitors (Phosphatase inhibitor Cocktail 2 and 3, Sigma-Aldrich) and 1 mmol/L Na_3VO_4, as described previously [4]. H9c2 and NCM extracts were collected by scraping cells in the same RIPA buffer described for LV proteins above.

Protein concentrations were determined with a Bradford-based method protein assay (Biorad, Marnes-la-Coquette, France) and samples were kept at −80 °C.

2.5. Phosphoproteomic screening

Two-dimensional (2D) gel electrophoresis was performed as previously described [3]. LV proteins (500 μg) from control (n=4) and HF (n=4) rats at 2 months after surgery were analysed on a dry 24-cm strip with a pH linear gradient of 3–10 (Immobilin DryStrip, GE Healthcare). Fluorescent staining of 2-D gel was performed with Pro-Q®Diamond Phosphoprotein Gel Stain (Molecular Probes™) for 90 min for detecting the phosphorylated proteins by image acquisation with an Ettan Dige Imager (GE Healthcare) at an excitation wavelength of 540 nm and an emission wavelength of 595 nm. Gels were then stained for total proteins with Sypro®Ruby Protein Gel Stain (Molecular Probes™) overnight and images of Sypro®Ruby stained gels were acquired with the Ettan Dige Imager at an excitation wavelength of 480 nm and an emission wavelength of 530 nm. Identification of spots of interest (spots 5 and 45) was performed by MALDI-TOF. Detailed methods have already been described [4].

2.6. Antibodies

Three primary antibodies against desmin were used, clone Y66 (ab32362, Abcam Paris, France), clone DE-U-10 (D1033, Sigma-Aldrich, Lyon, France) and clone D33 (M0760, Dako, Les Ulis, France) and one primary antibody against GAPDH (sc-365062, Santa Cruz) was used to confirm equal total proteins loads. The secondary antibody, ECL™ anti-mouse and rabbit IgG horseradish peroxidase-linked whole antibodies from sheep and donkey, respectively (GE Healthcare, Velizy-Villacoublay, France) was used for western blot. Alexa Fluor® 488 coupled anti-mouse and rabbit secondary antibodies (Invitrogen, Life Technologies) was used for immunofluorescence studies.
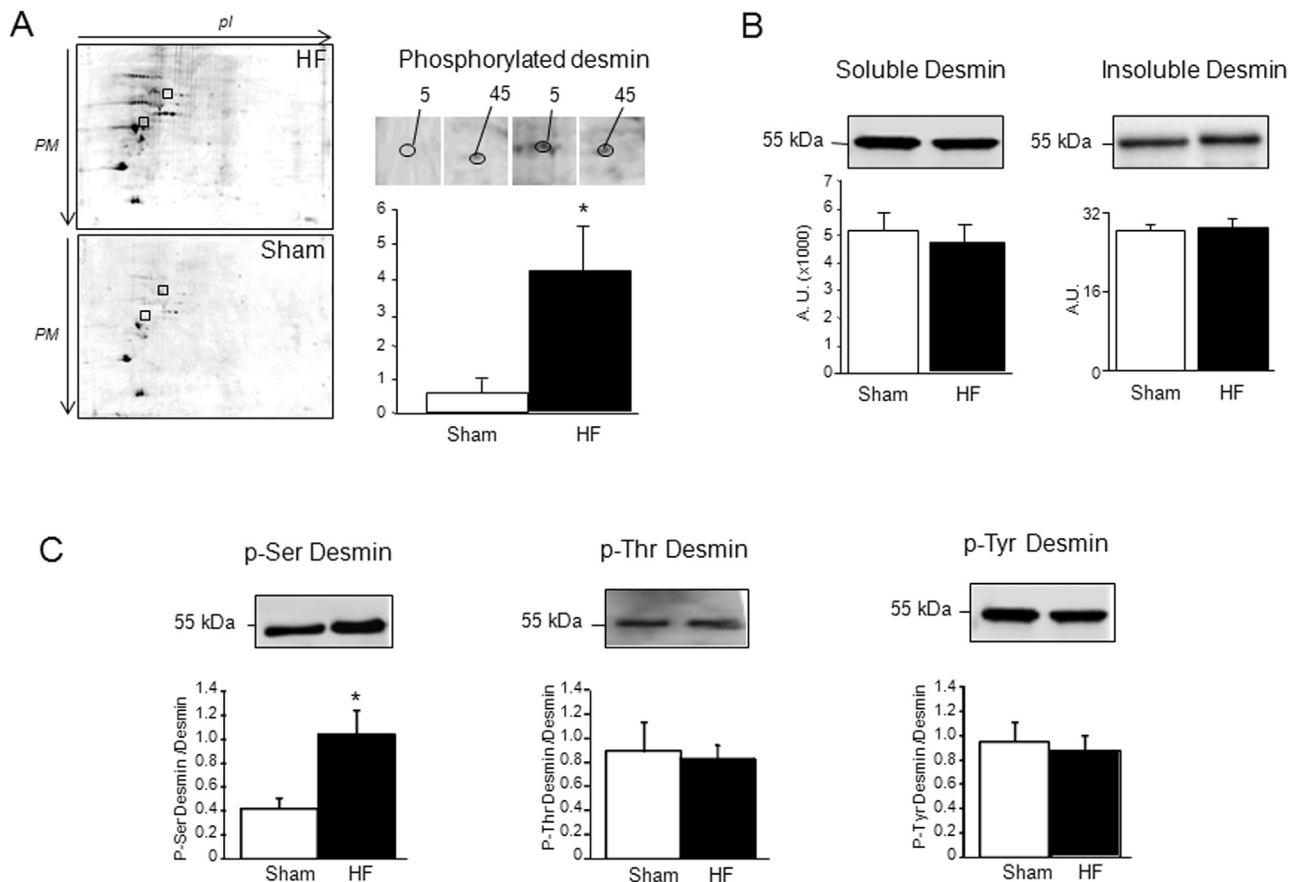
Fig. 1. Phosphoproteomic analysis of LV of HF rats. A: Representative 2D-electophoresis gel of LV proteins from HF (n=4) and sham-rats (n=4) stained with ProQDiamond®. The two polypeptidic spots identified to be desmin were enlarged and data of modulation of phosphorylated polypeptidic spots (5 and 45) are expressed as mean of normalized spot's volume ± SEM of normalized volume of total spots from sham (white box) and MI (black box)rats at 2 months.*P, 0.05. B: Quantification of desmin (soluble and insoluble fractions) levels in LV (50 μg) of sham- (n=11) (white box) and HF- (n=11) (black box) rats at 2 months after MI. Soluble and insoluble desmin were respectively quantified in LV proteins extracted in RIPA buffer (50 μg proteins) and Urea/Thiourea buffer (20 μg proteins). C: Ser-phosphorylated, Thr-phosphorylated and Tyr-phosphorylated desmin were quantified in LV (50 μg) of sham- (n=16) (white box) and HF- (n=19) (black box) rats at 2 months after MI. Data are presented as ratio of Ser-, Thr- and Tyr-phosphorylated desmin/total soluble desmin. The positions of Mw are indicated on the left. An internal standard was loaded in each gel for the standardization and quantification. Data are expressed as means of an arbitrary unit (AU) ± SEM.*P, 0.05.

2.7. Immunoprecipitation, western blot and PHOS-tag gels

2.7.1. Immunoprecipitation

Immunoprecipitation was performed with 50 μg of LV proteins, 2 μL of crude plasma and 75 μg of depleted- and CPLL-treated plasma, mixed with 2 μL of anti-desmin clone DE-U-10 (Sigma-Aldrich, Lyon, France) diluted in RIPA buffer. After an overnight incubation at 4 °C on a rotating device, immune complexes were precipitated at 4 °C for 4 h on a rotating device with protein A/G magnetic beads (Pierce). Immunoprecipitated (IP) complexes were then washed three times with RIPA buffer before extraction in Laemmli buffer at room temperature for western blot analysis.

2.7.2. Western blot

Western blot detection of desmin was performed with the three primary antibodies (1/2000). Briefly, 50 μg of soluble proteins (unless otherwise stated), 10 μg of insoluble proteins, 1 μL of crude plasma proteins, 50 μg of of depleted- and CPLL-treated plasma or the whole IP were resolved on 10% SDS-PAGE (NuPAGE 10% Bis-Tris gel, Life Technologies) and transferred on 0.2 μm nitrocellulose membranes (Trans-Blot® Turbo™ Transfert Pack, Bio-Rad). Equal total proteins loads were confirmed by Ponceau red [0.1% Ponceau red, 5% acetic acid (v/v) (Sigma-Aldrich)] staining of the membranes. The membranes were then blocked in 5% non-fat dry milk in TBS-Tween buffer for 1 h before 4 °C overnight incubation with desmin antibodies in blocking solution. Blots were then washed three times with TBS-Tween 0.1%

buffer and incubated with horseradish peroxidase-labelled secondary antibodies for 1 h (1/10000) in blocking solution. The Chemidoc® camera (Biorad) was used for imaging and densitometry analysis after membranes were incubated with enhanced chemiluminescence (ECL™) western blotting detection reagents (Biorad).

2.7.3. PHOS-TAG gels

Fifty μg of soluble LV proteins were separated in 10% Super-Sep™ Phos-tag™ 50 μM (Wako) at 90 V for 2 h 30 min. After electrophoretic separation, the excess of metal was removed by washing the gels twice for 10 min in transfer buffer (NuPAGE® Transfer Buffer, Invitrogen) containing 10% methanol and 10 mmol/L EDTA. Before proteins transfer onto 0.2 μm PVDF membrane (Trans-Blot® Turbo™ Transfer Pack, Bio-Rad), three washes of 10 min in transfer buffer containing only 10% methanol were realized. To detect desmin and its phosphorylated forms, membranes were blocked 1 h in 5% non-fat dry milk in TBS-Tween before overnight incubation at 4 °C with desmin clone DE-U-10 antibody (Sigma) at 1/1000 in blocking solution. The following steps were similar to those described in western blot section.

2.8. Immunofluorescence

Biphotonic confocal microscopy was used for the imaging of 4% paraformaldehyde and 0.1% Triton fixed/permeabilized NCMs and frozen rat heart sections (10 μm). Immunofluorescence staining
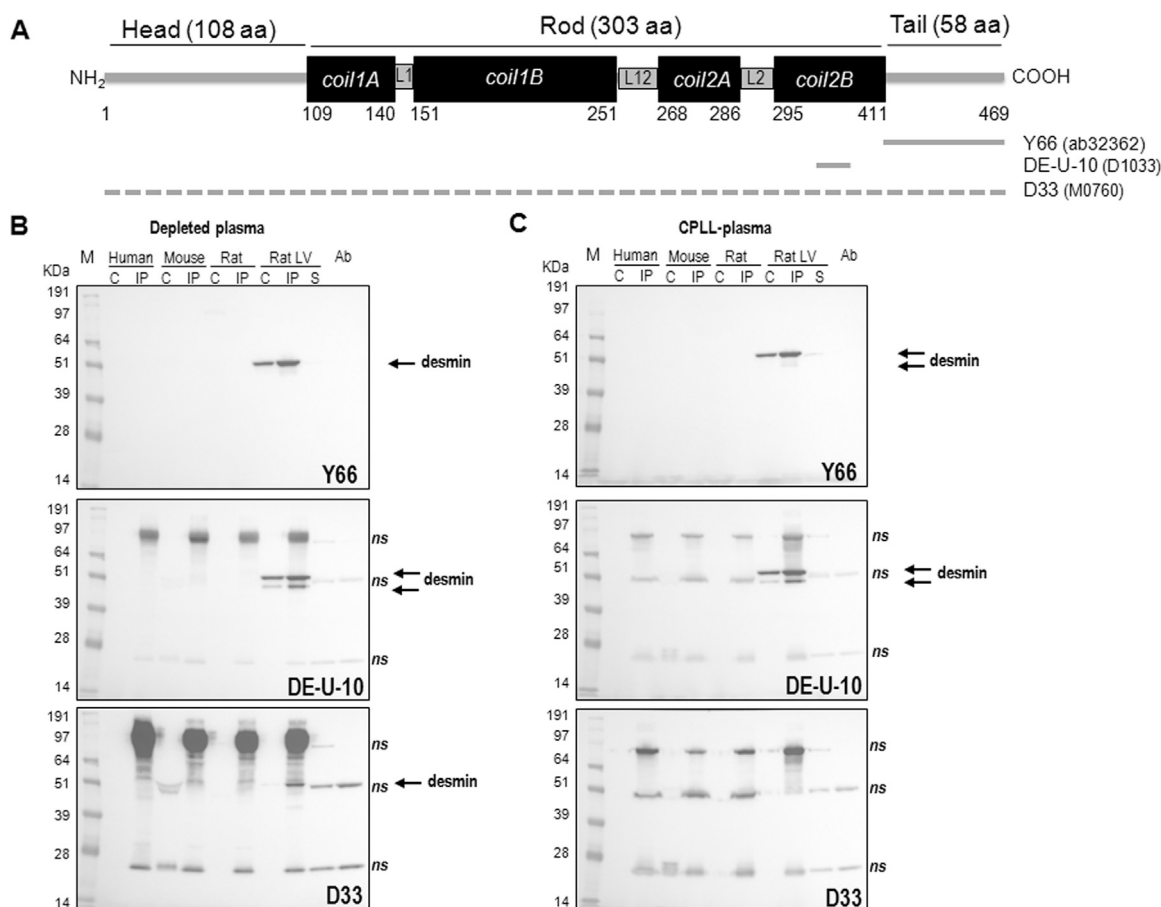
Fig. 2. A: Structural molecular organization of the rat desmin molecule (P48675) (adapted from [24] and desmin sequence recognized by the three desmin antibodies (clones Y66 (Abcam, ab32362), DE-U-10 (Sigma-Aldrich, D1033) and D33 (Dako, M0760) used for western blot. A dashed line is shown for the D33 antibody as no information on the epitope recognized is available. B, C: Western blot analysis of desmin in plasma from rat, mouse and human species with the three desmin antibodies. Plasma was either depleted for albumin and IgG (B) or treated by combinatorial peptide ligand library (CPLL) (C). M: size marker, C: 50 μg of treated plasma, IP: immunoprecipitated treated plasma with 2 μL of DE-U-10 desmin antibody, LV: left ventricle (10 μg), S: supernatant of LV IP (10 μg), Ab: antibody (2 μL). The antibody used for the western blot is indicated on each blot. Arrows indicate the specific desmin band recognized by the antibodies and ***ns*** the non-specific bands.

was performed by saturation for 30 min with 1% BSA before incubation with the three primary antibodies (dilution 1/100) against desmin overnight at 4 °C. Alexa Fluor® 555 coupled anti-mouse and rabbit secondary antibodies at dilution 1/500 was incubated for 30 min at room temperature with mounting medium (H-1500, Vectashield, Vector). Staining was visualized with the × 40 and × 63 objectives of LSM710 confocal microscope followed by Zen image acquisition and software analysis (Zeiss). Images were acquired with a resolution of at least 1024 × 1024.

2.9. Mass spectrometry analysis

2.9.1. 1D SDS-PAGE and digestion of proteins

Forty μg of proteins were denatured with Laemmli sample buffer (v/v), loaded onto 1D SDS-PAGE (12%) using 2 mm-stacking gel, and run for 10 min in order to concentrate the proteins before staining with colloidal coomassie G-250 (Bio-Rad). A slice per sample was excised, cut in small pieces (1 mm^3) and washed twice with 120 μl of 25 mmol/L ammonium bicarbonate (NH_5CO_3)/acetonitrile (ACN), before dehydration with 100 μl ACN for 5 min. Prior to digestion, the gel bands were reduced with 10 mmol/L DTT, alkylated with 50 mmol/L iodoacetamide (IAA) and digested with 0.4 μg of sequencing grade porcine trypsin (Promega, Madison, WI) for 16 h. The peptides were extracted with 25 mmol/L of NH_5CO_3/ACN (v/v) in 0.1% formic acid (FA), dried with vacuum concentration centrifuge (Uniequip GmbH, Munich, Germany) and resuspended in 12 μl of 0.1% FA.

2.9.2. Liquid chromatography and mass spectrometry analyses

Nano-LC analyses were performed on an Ultimate® 3000 RSLCnano System (Dionex/Thermo Scientific). Each sample (3 μl) was loaded into a trap column (Acclaim PepMap, 5 mm × 300 μm inner diameter, C_{18}, 5 μm, 100 Å), Dionex, Sunnyvale, CA) at 5 μl/min in 0.1% FA and 2% ACN for 5 min. The peptides were then concentrated on an analytical column (Acclaim PepMap RSLC, 15 cm × 75 μm inner diameter, C_{18}, 2 μm, 100 Å, Dionex) by a solvent A (0.1% FA in HPLC grade water) and a solvent B (0.1% FA in HPLC grade ACN) at a flow rate of 300 nl/min. Peptides were then eluted using a C18 analytical column and a 2 − 40% linear gradient of solvent B for 46 min followed by a washing step (6 min of 80% solvent B) at a flow rate of 300 nl/m.

2.9.3. Mass spectrometry analyses and protein identification

Eluted peptides from the C18 analytical column were analysed by a Q-Exactive mass spectrometer (Thermo Scientific, Bremen, Germany) with a spray voltage et up at 1.9 kV, and capillary temperature set up at 275 °C. Data acquisition was performed in a data-independent mode consisting of a full scan MS over the range m/z 230–2000 with resolution of 70,000 at m/z 200 and a full scan MS/MS of the ten most intense peaks. MS/MS data were acquired using a 2 m/z units ion isolation window and a collision energy of 24. These experiments performed in triplicate for each sample were fully controlled by Thermo Xcalibur 3.0 (Thermo Fisher Scientific).

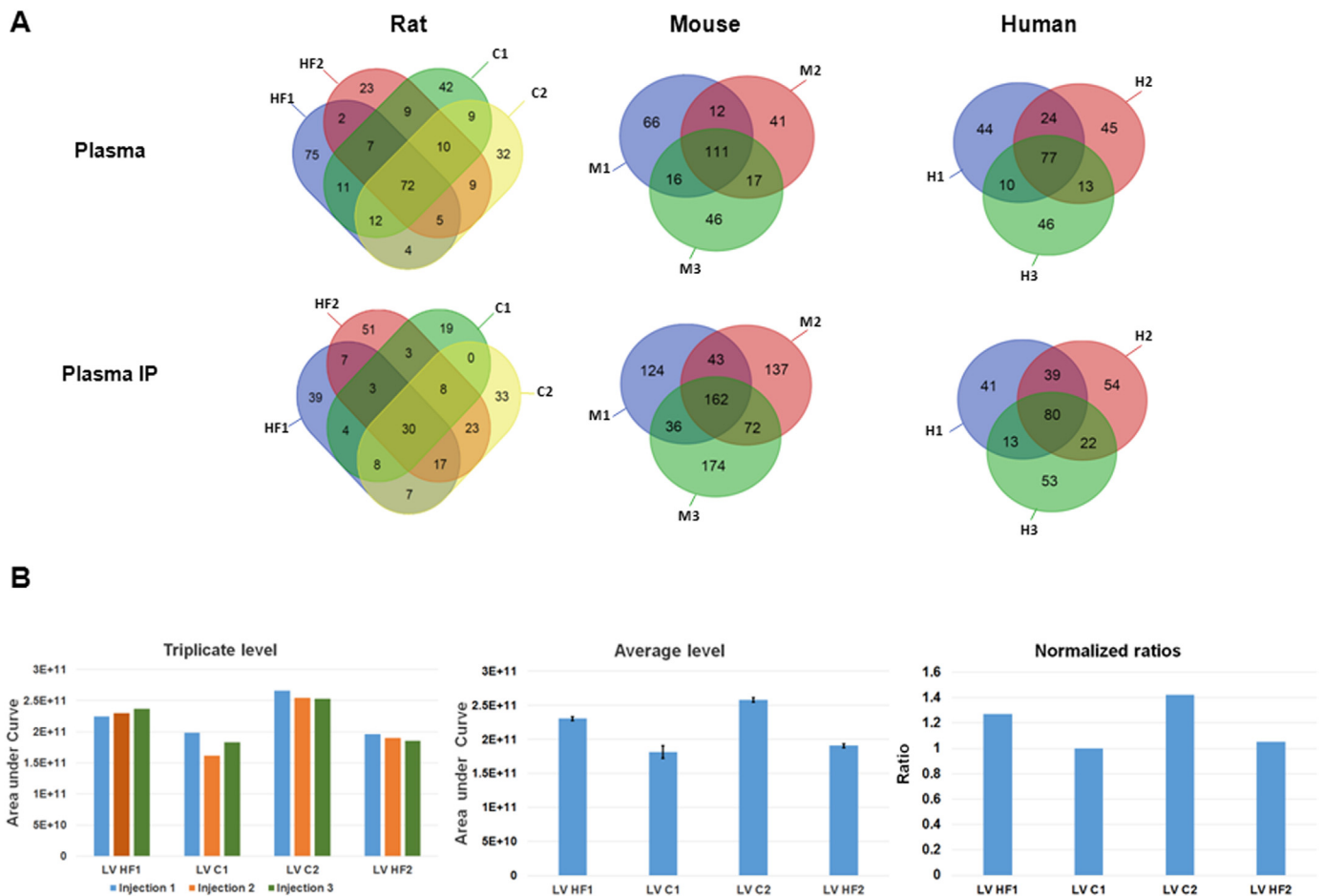All data files (*.raw) collected during nanoLC-MS/MS analyses

Fig. 3. Mass spectrometry analysis of rat, mouse and human plasma (A) and rat LV (B) samples. A: Venn diagram of identified proteins in crude plasma (upper panel) and plasma immunoprecipitated with DE-U-10 desmin antibody (lower panel). For plasma, 4 samples from 2 HF- (HF1, HF2) and 2 sham- (C1, C2) rats, 3 different samples from mouse (M1, M2, M3) and human (H1, H2, H3) were analysed. B: Quantification of desmin in LV samples corresponding to the rats tested for plasma (HF1, HF2, C1, and C2). Levels of the 3 replicates injection of each sample show the reproducibility (left panel). Average levels of desmin in LV rats with standard deviation less than 10% (middle panel). Ratio levels of desmin in LV rats with the sham-C1 rats considered as the lower level for the ratio calculation (right panel). Detailed information's are presented in Table 1.

were processed with a workflow designed in Proteome Discoverer 1.4 (Thermo Fisher Scientific). The MS/MS spectra were filtered with 1.5 signal-to-noises (S/N) threshold. Tryptic monoisotopic peptide masses were searched for in the National Center of Biotechnology Information (*Homo sapiens* protein sequences (118,210 entries), *Rattus norvegicus* protein sequences (84,085 entries) and *Mus musculus* protein sequences (174,503 entries)) using Mascot (Version 2.4.1, Matrix Science, London, UK) and Sequest HT (Thermo Fisher Scientific) with a mass tolerance of 10 ppm for precursor ions and 0.02 Da for fragment ions and 3 missed cleavages per tryptic peptide. Chemical modifications such as carbamidomethylation (cysteine), acetylation of N-terminal protein, oxidation (methionine) and deamidation (glutamine, asparagine) were taken into consideration. The criteria to accept identification included a score of probability greater than 25 for Mascot and greater than 2 for Sequest HT XCorr. The target-decoy database search allowed us to verify and estimate the false positive identification rate of our study below 1% [18].

2.9.4. Label-free quantification of desmin
Desmin abundance was quantified by calculating the area under the curve for each precursor ion identified as a peptide mapping to desmin at 2 ppm with Proteome Discoverer. The average level was calculated as the mean value of the area obtained for each identified peptide in the three replicates. The

ratios of desmin were normalized with the sample containing the lowest amount of desmin.

2.10. Statistical analysis

Data are expressed as means $\pm$ SEM. Statistical analysis of the cardiac functional parameters was performed by the Wilcoxon test. For the other analyses, an unpaired *t*-test was used to evaluate differences between groups. A value of $P < 0.05$ was considered statistically significant.

3. 3. Results

3.1. Levels of desmin and its phosphorylated forms in left ventricle of rats with heart failure

By phosphoproteomic screening performed in LV of HF-rats compared to sham-rats, we previously detected 69 polypeptidic spots and identified 30 different proteins with modulation of their phosphorylation level (Supplemental Fig. 1 and [4]). We focused on two spots labelled 5 and 45 presented on enlarged 2D (Fig. 1A) that showed an increase (by a mean factor of 4) in phosphorylation in the LV of sham-rats compared to the HF rats (spot 5:0 *vs* 3.26 $\pm$ 2.27 and spot 45:0.89 $\pm$ 0.52 *vs* 1.19 $\pm$ 0.72 A.U.). The two

Table 1
Summary of desmin identification in the 4 different rat LV samples (HF1, HF2, C1 and C2).

	Sample	HF1	HF2	C1	C2
∑ **coverage**	Left ventricle	91%	91%	91%	92%
	LV IP	91%	97%	94%	94%
	Plasma	–	–	–	–
	PI IP	–	–	–	–
∑ **unique peptides**	Left ventricle	56	58	54	60
	LV IP	69	78	75	78
	Plasma	–	–	–	–
	PI IP	–	–	–	–
∑ **peptides**	Left ventricle	62	64	58	68
	LV IP	75	84	82	83
	Plasma	–	–	–	–
	PI IP	–	–	–	–
Mascot/Sequest PSMs	Left ventricle	1867/ 2628	1476/ 2102	1384/ 2239	1853/ 2805
	LV IP	2621/ 2967	2542/ 3248	2912/ 3706	3283/ 4918
	Plasma	–	–	–	–
	PI IP	–	–	–	–

LV IP: left ventricle immunoprecipitated with desmin antibody, PL IP, plasma immunoprecipitated with desmin antibody, HF: heart failure, C: control, ∑ coverage: total percentage of the protein sequence covered by identified peptides (combined Mascot and Sequest analyses), ∑ unique peptides: Total number of peptide sequences unique to a protein (combined Mascot and Sequest analyses), ∑ peptides: Total number of distinct peptide sequences identified in the protein (combined Mascot and Sequest analyses), PSMs: Total number of identified peptide sequences (peptide spectrum matches),-: no identification of desmin.

spots were identified as being desmin (Supplemental Table 1).

As previously shown, no detection of modulation of desmin levels in LV of HF rats was observed during the previous proteomic screening [3]. These previous data were confirmed here by western blot using an antibody specific to desmin in both soluble (RIPA extracts) and insoluble (thiourea/urea extracts) (Fig. 1B).

We then looked for the amino acids (Ser, Thr and Tyr) involved in the increased phosphorylation of desmin and observed that desmin was phosphorylated on Serine (Ser), Threonine (Thr) and Tyrosine (Tyr) but only the phosphorylation of desmin on Ser was modulated in the LV of HF- compared to the sham-rats (Fig. 1C). We verified the specificity of the Ser-phosphorylation by treatment of the LV proteins with alkaline phosphatase, leading to the complete cleavage of phosphorylation and consequently to an absence of signal (not shown).

3.2. Levels of desmin in plasma

To verify for the presence of desmin in plasma, we used different antibodies from 3 different clones that recognized both human, rat and mouse species (Fig. 2A). The desmin antibodies (clone Y66, raised in rabbit and used in Fig. 1 and clone DE-U-10, raised in mouse) recognized the C-terminal part of the sequence corresponding respectively to the desmin tail (412–469 AA) and the Col2B region (325–372 AA). The third one (clone D33, raised in mouse) was previously used for detecting desmin in heart and plasma from mouse and human species [6].

First, we analysed crude plasma from rats and humans for the presence of desmin and did not find any specific bands (data not shown). We then treated plasma from rat, mouse and human species either for CPPL or Alb/IgG depletion in order to access low-abundance proteins that we analysed directly or after immunoprecipitation (IP) with the desmin antibody (clone DE-U-10) to increase the sensitivity of detection. We observed different western blots either at short (Fig. 2B–C) and long exposure (Supplemental Fig. 2) performed with the three different antibodies. The Y66 antibody, produced in rabbit, which recognizes the

C-terminal part of desmin, has the best specificity as shown by the specific band detected in crude and IP LV proteins at 53 kDa (arrow) and no band detected in supernatant of IP at short exposure or with the antibody loaded, which was used for the immunoprecipitation of desmin. But, we were unable to detect specifically desmin in the plasma of any species either after CPPL or Alb/IgG depletion with this antibody. The DE-U-10 desmin antibody recognized only desmin in LV proteins. The bands detected in plasma were all unspecific (Supplemental Fig. 2). Surprisingly, the D33 antibody which was raised against the same full length desmin sequence as the DE-U-10 antibody was less sensitive and less specific with the highest background detected at short exposure (Fig. 2B–C) and detection of desmin only in crude LV at long exposure (Supplemental Fig. 2). We have also verified the specificity of IP without antibody, showing that desmin was detected in the supernatant IP (corresponding to the unbound proteins) and not in the IP (bound proteins) by western blot with the DE-U-10 desmin antibody (Supplemental Fig. 3).

To ensure the absence of desmin in plasma, we also perform mass spectrometry analysis of crude and plasma immunoprecipitated with the DE-U-10 desmin antibody (Fig. 3A) from rat, mouse and human species. We used LV proteins as positive control to ensure recovery of the eluted desmin peptides (Fig. 3B). In any of crude or IP plasma samples (rat (n=4), mouse (n=3) and human (n=3) samples), no desmin peptides were detected despite a high number of peptides identified (322 in rat, 309 in mouse and 259 in human samples) (Fig. 3A). Conversely, the same MS approach used with LV proteins has identified desmin successively and reproducibly with sequence coverage of more than 90% (Fig. 3B, Table 1). Interestingly, by this approach we have identified the aminoacids phosphorylated in LV of the rat model of ischemic HF to be the serine 25, 28, 31, 32, 60, 68, 81, 91, 329, 343 and 431 (Supplemental Fig. 4).

3.3. Biochemical characterization of desmin

To understand why desmin is not detected in plasma, suggesting that desmin is not secreted from cardiomyocytes into the blood, we characterized the level of desmin upon cell fractionation. Desmin level was analysed in soluble (RIPA buffer) and insoluble (urea/thiourea buffer) fraction extracted from LV of sham- and HF-rats. At short exposure, we observed that most of desmin was detected in the insoluble fraction of LV proteins and interestingly a lower molecular weight band was detected in HF rat (Fig. 4A), as already shown with the DE-U-10 antibody (Fig. 2B–C). Interestingly, the same profile was observed with two desmin antibodies (DE-U-10, upper panel and Y66, lower panel in Fig. 4A).

To determine if there is any difference in non-phosphorylated/phosphorylated desmin patterns depending on the soluble/insoluble fraction, we used the phosphate affinity SDS-PAGE (Phostag™), which has the properties to delay phosphoproteins during electrophoresis, thus allowing the separation of the phosphorylated (mono-, bis-, or more) forms from their unphosphorylated form according to their number of phosphate moieties. We did not observe any significant differences in unphosphorylated or phosphorylated forms of desmin either in soluble fraction or insoluble fraction of LV proteins independently of the amount of desmin detected which is rather low in soluble fraction compared to insoluble fraction (Fig. 4B).

Finally, we characterize the subcellular localization of desmin by immunofluorescence in NCMs and rat LV (Fig. 5). Interestingly, the desmin stainings in NCMs (Fig. 5A–C) and LV (Fig. 5D–F) were different depending on the desmin antibodies. The Y66 and DE-U-10 antibodies detected desmin in intermediate filaments both in NCMs (Fig. 5A–B) and LV (Fig. 5D–E). The D33 antibody gave a completely different staining for desmin in NCMs (Fig. 5C) and
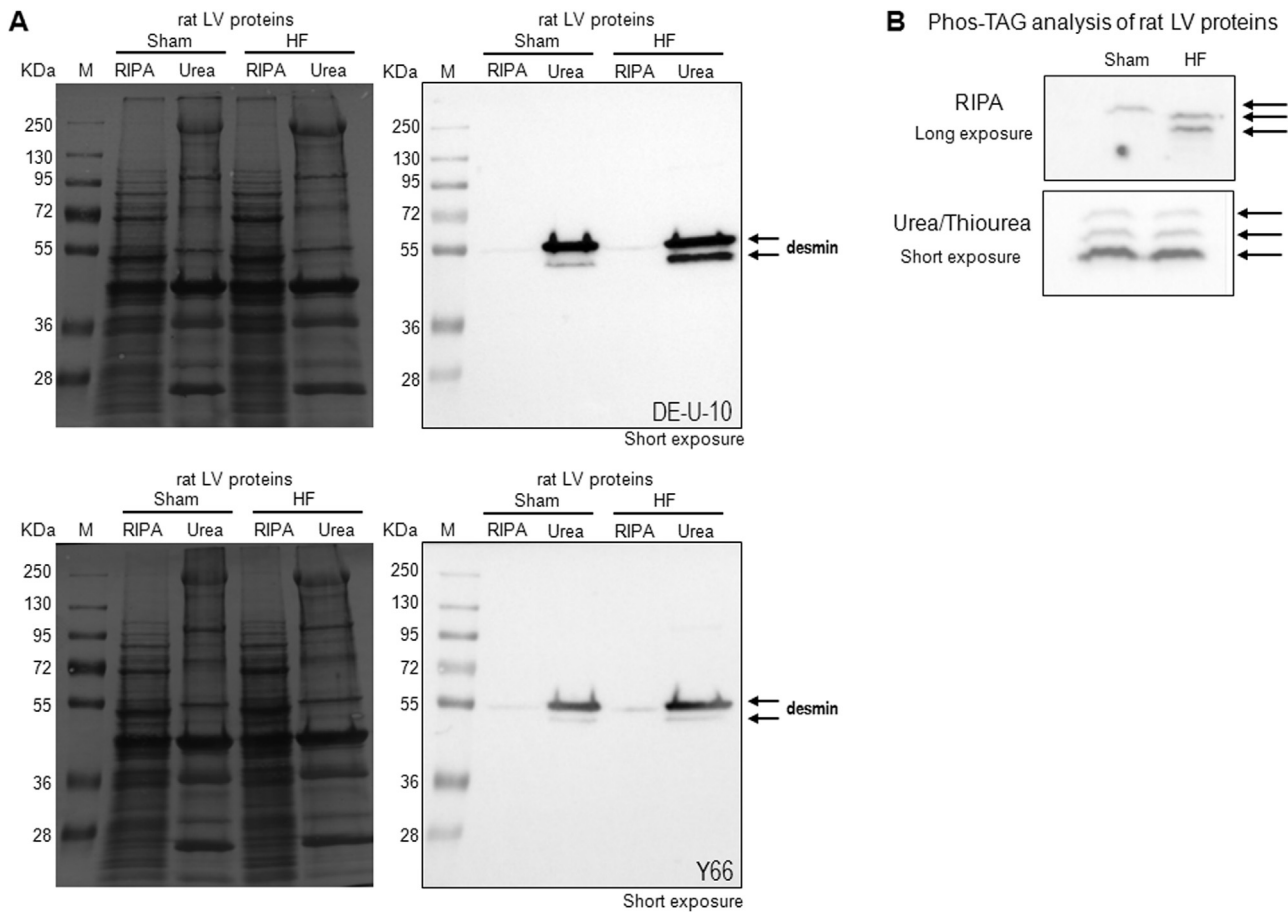
Fig. 4. Biochemical characterization of desmin. A**:** Western blot analysis of desmin in LV proteins (50 μg) extracted from sham- and HF-rats in RIPA and Urea/Thiourea buffer. The ponceau red staining gel (left panel) and the western blot images (right panel) with desmin DE-U-10 (upper panel) and Y66 (lower panel) antibodies at short exposure are presented. B: Western blot analysis of desmin in LV proteins separated using Phos-Tag (8%, 50 μmol/L) affinity electrophoresis performed with the DE-U-10 antibody. LV proteins are extracted in RIPA (50 μg of proteins) (upper panel) or Urea/Thiourea (20 μg of proteins) (lower panel) buffer. The western blot images presented are at long exposure (> 1000 s) for RIPA extraction and short exposure (12 s) for Urea/Thiourea extraction. Arrows indicate the specific desmin bands recognized. M: size marker.

only few desmin staining in intermediate filaments LV (Fig. 5F). These data strengthened the different patterns obtained by western blots performed with the different desmin antibodies (Fig. 2).

4. Discussion

In the present study, we found a 2-fold increased phosphorylation of desmin levels by phosphoproteomic analysis in a well characterized rat ischemic HF experimental model in which the induction of anterior MI leads to LV remodeling and to HF [14]. We aimed to investigate 1) the behavior of phosphorylated desmin because post-translational modifications of desmin has been shown to cause disturbance of intermediate skeletal network [19] and, 2) the potential of phosphorylated desmin as biomarker of events linked to ischemic HF as desmin was recently shown to be present in plasma [6].

As shown previously [3], we did not find any modulation of total desmin either in soluble or insoluble fractions of LV proteins in our model of impaired systolic heart function. Various behavior of desmin has been shown depending upon the experimental animal models of HF used. Our data are in accordance with those recently published in a canine pacing model of desynchronous HF, characterized by pressure overload, showing increased levels of phosphorylated desmin [20]. Interestingly, it was recently shown in two different mice models, one of diastolic dysfunction obtained by transverse aortic constriction [21] and the other one, the

transgenic calcineurin model, characterized by a phenotype of end stage heart failure [6], an up-regulation of desmin with no proportional increase in phosphorylation.

We also identified that most of the phosphorylated desmin was present in the insoluble fraction of LV, suggesting the formation of desmin aggregates in failing heart, as described in desminopathies in which desmin causative mutations led to the accumulation of insoluble desmin-containing aggregates, and destructive changes in the sarcomere [22]. By mass spectrometry, we have identified new serines to be phosphorylated and confirmed the Ser 28 and 32 (rat species) already described in different experimental models [20,23].

Pathological hyperphosphorylation of IF is frequently accompanied by IFs reorganization and aggregation [19]. Desmin is considered as a major integrator of contractile apparatus to the nucleus and other organelles and is a critical factor for maintaining IFs structure. Its increased phosphorylation might lead to the network destabilization and formation of aggregates toxic for the cardiomyocyte [7]. Our phosphoproteomic data have also shown two 2D spots with different Mw and *pI* identified as being desmin in accordance with the multiple desmin species detected in a model of hypertrophied cardiomyocytes [24]. These multiple desmin species has been suggested to be products of cleavage by a Ca^{2+}-activated proteinase [25], which was characterized later as being calpain [26]. Interestingly, calpains play a critical role in heart protein homeostasis and are activated during HF
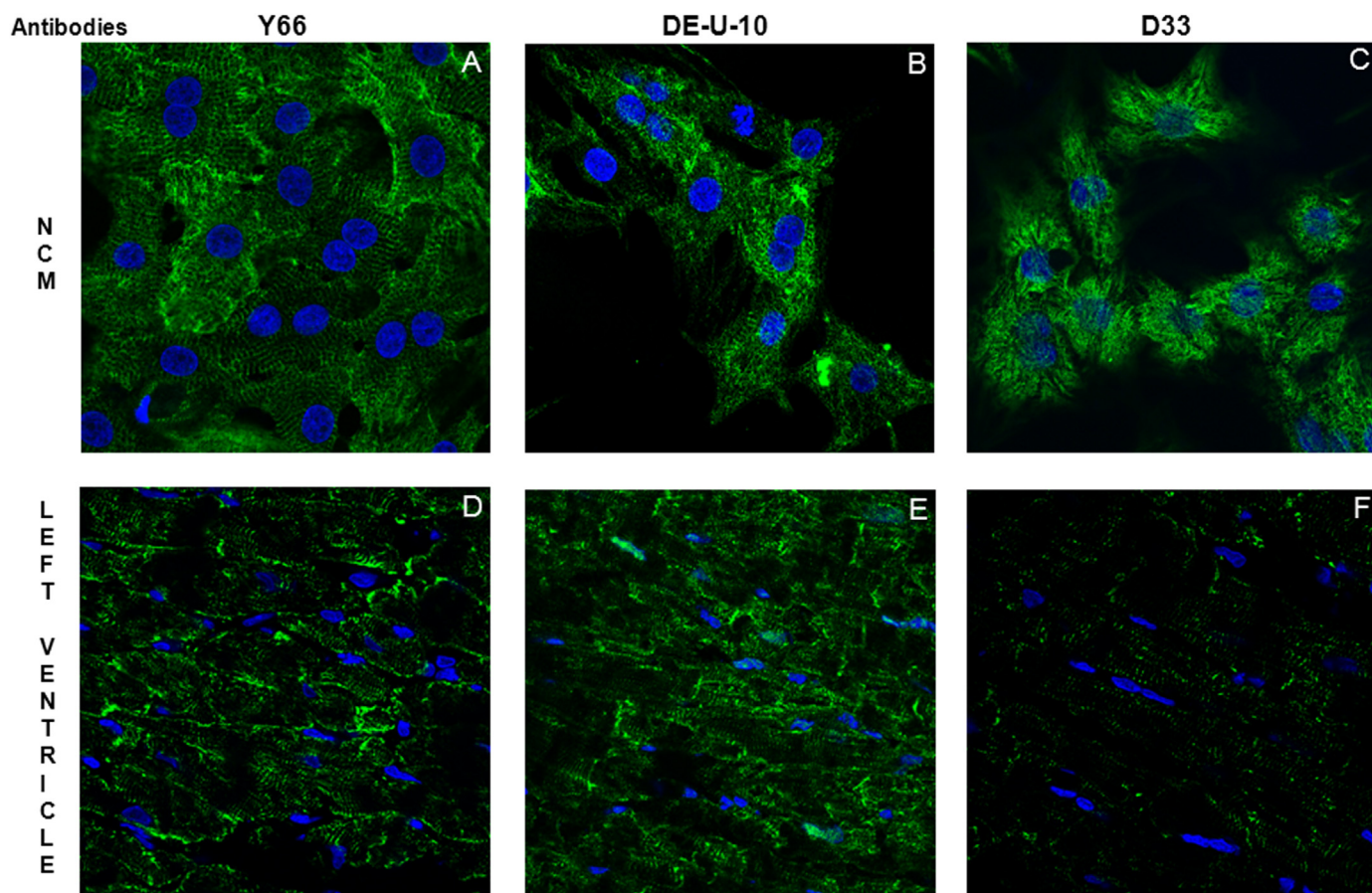
Fig. 5. Representative immunofluorescence stainings of desmin (green) in primary culture of neonate rat cardiomyocytes (NCM) (A, B, C) and in left ventricle from control rat (D, E, F) with the three desmin antibodies. Nuclei are stained in blue (DAPI).

development [8]. The lower desmin band detected by western blot might be a proteolytic cleavage of desmin by calpain (TRAP in position 76–80 which is a pig desmin fragment obtained after incubation by calpains and analysed by N-terminal sequencing [26]. These cleavages are located in the head domain of the desmin whose aminoacid sequence is conserved in rat, mouse, pig and human species (supplemental Fig. 4). This is in accordance with previous description of 2 isoforms of desmin in endomyocardial biopsies from familial HF patients [27].

We may speculate that the increased phosphorylation of desmin induced increased desmin cleavage by calpain in order to protect cardiomyocytes from the aggregates. Calpain is required for localized cytoskeleton remodeling at injury sites and plasma membrane maintenance under hemodynamic stress [8]. This activation of calpains at injured sites leads to proteolysis of desmin for clearance and membrane repair (patch vesicle). Desmin degradation products upon damage and processing by calpain might be at the origin of desmin in plasma. We could not exclude that the presence of phosphorylation sites may impact the susceptibility of desmin to cleavage. It was shown with a missense mutation in desmin tail domain, the existence of interplay between the head and tail domain that may affect the susceptibility of desmin to specific proteases and abolish its Z-disc localization [28]. But contrarily to a previous publication [6], we were unable to detect desmin in plasma of mouse, rat and human despite the use of several desmin antibodies and a sensitive mass spectrometry analyses.

5. Conclusions

From our data and others, we speculate that the increased phosphorylated form of desmin detected in ischemic HF increased susceptibility of desmin to proteolysis, resulting in desmin degradation products through calpain-mediated cleavage. The next step requires using calpain inhibitors or cells deficient in calpain in order to explore and identify precisely the specificity and the sites of desmin cleavages. Contrarily to others [6], we were unable to detect specifically desmin in plasma from different species. We should not exclude that in late/aggravated stages of HF of non-ischemic origin, such as the model of 14 weeks-old calcineurin transgenic mice, cleaved forms of desmin can be released passively from the heart due to disruption of architecture. In a TNF-induced mice model of cardiomyopathy, desmin was shown to be cleaved by caspase 6 revealing 24 and 29 kDa fragments in heart, which may be responsible for a loss of intercalated disk localization [29]. Interestingly, it was shown that the desmin expression and pattern of striation by immunostaining correlated with the level of myocardial injury in patients with idiopathic dilated cardiomyopathy and may be used a marker of HF progression [30].

Deciphering the functional serine(s) involved in the hyperphosphorylation of desmin during the cardiac remodeling process following MI will be important with the purpose of developing specific tools, such as antibodies against the serine-phosphorylated desmin in order to detect phosphorylated-desmin degradation products and study the behavior of desmin, such as its localization to Z-disc or aggregate formation. Future studies will need to characterize the utility of post-translational modifications as

circulating or tissue biomarkers and the targets involving IFs proteins [31].

Funding sources

This work was supported by grants from the National Agency for Research (ANR), ANR blanc–SVSE1 (ANR-10-BLAN-1104), the E. U. FP7 HOMAGE (305,507), the Laboratoire d'Excellence (LabEx) ParaFrap from ANR, ANR-11-LABX-0024, the "Fonds Européen de Développement Economique Régional" (FEDER), the "Métropole Européenne de Lille" (MEL) and the "Région Nord Pas de Calais".

Conflict of interest

None.

Acknowledgments

We thank Jean-Paul Henry for the surgical induction of MI.

Appendix A. Supporting information

Supplementary data associated with this article can be found in the online version at http://dx.doi.org/10.1016/j.bbrep.2016.02.014.

References

[1] A.S. Go, D. Mozaffarian, V.L. Roger, E.J. Benjamin, J.D. Berry, M.J. Blaha, S. Dai, E. S. Ford, C.S. Fox, S. Franco, H.J. Fullerton, C. Gillespie, S.M. Hailpern, J.A. Heit, V. J. Howard, M.D. Huffman, S.E. Judd, B.M. Kissela, S.J. Kittner, D.T. Lackland, J. H. Lichtman, L.D. Lisabeth, R.H. Mackey, D.J. Magid, G.M. Marcus, A. Marelli, D. B. Matchar, D.K. McGuire, E.R. Mohler, 3rd, C.S. Moy, M.E. Mussolino, R. W. Neumar, G. Nichol, D.K. Pandey, N.P. Paynter, M.J. Reeves, P.D. Sorlie, J. Stein, A. Towfighi, T.N. Turan, S.S. Virani, N.D. Wong, D. Woo, M.B. Turnerl, American heart association statistics committee and stroke statistics sub-committee. Heart disease and stroke statistics-2014 update: a report from the American heart association, Circulation 129 (2014) e28–e292.
[2] M.L. Lindsey, M. Mayr, A.V. Gomes, C. Delles, D.K. Arrell, A.M. Murphy, R. A. Lange, C.E. Costello, Y.F. Jin, D.T. Laskowitz, F. Sam, A. Terzic, J. Van Eyk, P. R. Srinivas, Transformative impact of Proteomics on cardiovascular health and disease: a scientific statement from the American heart association, Circulation 132 (2015) 852–872.
[3] C. Cieniewski-Bernard, P. Mulder, J.P. Henry, H. Drobecq, E. Dubois, G. Pottiez, C. Thuillez, P. Amouyel, V. Richard, F. Pinet, Proteomic analysis of left ventricular remodeling in an experimental model of heart failure, J. Proteome Res. 7 (2008) 5004–5016.
[4] E. Dubois, V. Richard, P. Mulder, N. Lamblin, H. Drobecq, J.P. Henry, P. Amouyel, C. Thuillez, C. Bauters, F. Pinet, Decreased serine207 phosphorylation of troponin T as a biomarker for left ventricular remodelling after myocardial infarction, Eur. Heart J. 32 (2011) 115–123.
[5] E. Dubois-Deruy, A. Belliard, P. Mulder, M. Chwastyniak, O. Beseme, J.P. Henry, C. Thuillez, P. Amouyel, V. Richard, F. Pinet, Circulating plasma Ser208-phosphorylated troponin T levels are indicator of cardiac dysfunction, J. Cell. Mol. Med. 17 (2013) 1335–1344.
[6] S. Chugh, M. Ouzounian, Z. Lu, S. Mohamed, W. Li, N. Bousette, P.P. Liu, A. O. Gramolini, Pilot study identifying myosin heavy chain 7, desmin, insulin-like growth factor 7, and annexin A2 as circulating biomarkers of human heart failure, Proteomics 13 (2013) 2324–2334.
[7] J. Lowery, E.R. Kuczmarski, H. Herrmann, R.D. Goldman, Intermediate filaments play a pivotal role in regulating cell architecture and function, J. Biol. Chem. 290 (2015) 17145–17153.
[8] K. Nishida, O. Yamaguchi, K. Otsu, Degradation systems in heart failure, J. Mol. Cell. Cardiol. 84 (2015) 212–222.
[9] D.L. Winter, D. Paulin, M. Mericskay, Z. Li, Posttranslational modifications of desmin and their implication in biological processes and pathologies, Histochem. Cell. Biol. 141 (2014) 1–16.
[10] R.L. Mellgren, X. Huang, Fetuin A stabilizes m-calpain and facilitates plasma membrane repair, J. Biol. Chem. 282 (2007) 35868–35877.
[11] Q. Chen, E.J. Lesnefsky, Heart mitochondria and calpain 1: location, function, and targets, Biochim. Biophys. Acta 2015 (1852) 2372–2378.
[12] P. Mulder, V. Richard, G. Derumeaux, M. Hogie, J.P. Henry, F. Lallemand, P. Compagnon, B. Macé, E. Comoy, B. Letac, C. Thuillez, Role of endogenous endothelin in chronic heart failure: effect of long-term treatment with an endothelin antagonist on survival, hemodynamics, and cardiac remodeling, Circulation 96 (1997) 1976–1982.
[13] M.A. Pfeffer, J.M. Pfeffer, C. Steinberg, P. Finn, Survival after an experimental myocardial infarction: beneficial effects of long-term therapy with captopril, Circulation 72 (1985) 406–412.
[14] P. Mulder, S. Barbier, A. Chagraoui, V. Richard, J.P. Henry, F. Lallemand, S. Renet, G. Lerebours, F. Mahlberg-Gaudin, C. Thuillez, Long-term heart rate reduction induced by the selective I(f) current inhibitor ivabradine improves left ventricular function and intrinsic myocardial structure in congestive heart failure, Circulation 109 (2004) 1674–1679.
[15] E. Dubois-Deruy, A. Belliard, P. Mulder, M. Bouvet, C. Smet-Nocca, S. Janel, F. Lafont, O. Beseme, P. Amouyel, V. Richard, F. Pinet, Interplay between phosphorylation and O–N-acetylglucosaminylation of troponin T in ischaemic heart failure, Cardiovasc. Res. 107 (2015) 56–65.
[16] G. Lemesle, F. Maury, O. Beseme, L. Ovart, P. Amouyel, N. Lamblin, P. de Groote, C. Bauters, F. Pinet, Multi-marker proteomic profiling for the prediction of cardiovascular mortality in patients with chronic heart failure, PLOS One 10 (2015) e0119265.
[17] O. Beseme, M. Fertin, H. Drobecq, P. Amouyel, F. Pinet, Combinatorial peptide ligand library plasma treatment: advantages for accessing low-abundance proteins, Electrophoresis 31 (2010) 2697–26704.
[18] J.E. Elias, S.P. Gygi, Target-decoy search strategy for increased confidence in large-scale protein identifications by mass spectrometry, Nat. Methods 4 (2007) 207–214.
[19] Y. Capetanaki, S. Papathanasiou, A. Diokmetzidou, G. Vatsellas, M. Tsikitis, Desmin related disease: a matter of cell survival failure, Curr. Opin. Cell. Biol. 32 (2015) 113–120.
[20] G. Agnetti, V.L. Halperin, J.A. Kirk, K. Chakir, Y. Guo, L. Lund, F. Nicolini, T. Gherli, C. Guarnieri, C.M. Caldarera, G.F. Tomaselli, D.A. Kass, J.E. Van Eyk, Desmin modifications associate with amyloid-like oligomers deposition in heart failure, Cardiovasc. Res. 102 (2014) 24–34.
[21] J.J. Sheng, H.Z. Fengt, J.R. Pinto, H. Wei, J.P. Lin, Increases of desmin and α-actinin in mouse cardiac myofibrils as a response to diastolic dysfunction, J. Mol. Cell Cardiol. Oct. (31) (Epub ahead of print).
[22] D. Paulin, A. Huet, L. Khanamyrian, Z. Xue, Desminopathies in muscle disease, J. Pathol. 204 (2004) 418–427.
[23] N. Diguet, Y. Mallat, R. Ladouce, G. Clodic, A. Prola, E. Tritsch, J. Blanc, J. C. Larcher, C. Delcayre, J.L. Samuel, B. Friguet, G. Bolbach, Z. Li, M. Mericskay, Muscle creatine kinase deficiency triggers both actin depolymerization and Desmin disorganization by advanced glycation end products in dilated cardiomyopathy, J. Biol. Chem. 286 (2015) 35007–35019.
[24] G. Agnetti, K. Bezstarosti, D.H. Dekkers, A.J. Verhoeven, E. Giordano, C. Guarnieri, C.M. Caldarera, J.E. Van Eyk, J.M. Iamers, Proteomic profiling of endothelin-1-stimulated hypertrophic cardiomyocytes reveals the increase of four different desmin species and alpha-B- crystalline, Biochim. Biophys. Acta 2008 (1784) 1068–1076.
[25] W.J. Nelson, P. Traub, Purification and further characterization of the $Ca2^+$-activated proteinase specific for the intermediate filament proteins vimentin and desmin, J. Biol. Chem. 257 (1982) 5544–5553.
[26] C.P. Baron, S. Jacobsen, P.P. Purslow, Cleavage of desmin by cysteine proteases: calpains and cathepsin B, Meat Sci. 68 (2004) 447–456.
[27] E. Arbustini, P. Morbini, M. Grasso, R. Fasani, L. Verga, O. Bellini, B. Dal Bello, C. Campana, G. Piccolo, O. Febo, C. Opasich, A. Gavazzi, V.J. Ferrans, Restrictive cardiomyopathy, atrioventricular block and mild to subclinical myopathy in patients with desmin-immunoreactive material deposits, J. Am. Coll. Cardiol. 31 (1998) 645–653.
[28] M. Mavroidis, P. Panagopoulou, I. Kostavasili, N. Weisleder, Y. Capetanaki, A missense mutation in desmin tail domain linked to human dilated cardiomyopathy promotes cleavage of the head domain and abolishes its Z-disc localization, FASEB J. 9 (2008) 3318–3327.
[29] P. Panagopoulou, C.H. Davos, D.J. Milner, E. Varela, J. Cameron, D.J. Mann, Y. Capetanaki, Desmin mediates TNF-alpha-induced aggregate formation and intercalated disk reorganization in heart failure, J. Cell. Biol. 181 (2008) 761–775.
[30] A. Pawlak, R.J. Gil, T. Kulawik, M. Pronicki, A. Karkucińska-Więckowska, T. Szymańska-Dębińska, K. Gil, N. Lagwinski, E. Czarnowska, Type of desmin expression icardiomyocytes-a good marker of heart failure development in idiopathic dilated cardiomyopathy, J. Intern. Med. 272 (2012) 287–297.
[31] N.T. Snider, M.B. Omary, Post-translational modifications of intermediate filament proteins: mechanisms and function, Nat. Rev. Mol. Cell. Biol. 15 (2014) 163–177.